

Molecular Motions in Solid $[\text{Sb}(\text{CH}_3)_4]\text{PF}_6$. A Combined ^1H , ^{19}F Nuclear Magnetic Resonance and Quasielastic Neutron Scattering Study

Günter Burbach*, Norbert Weiden, and Alarich Weiss

Institut für Physikalische Chemie, Physikalische Chemie III, Technische Hochschule Darmstadt,
Darmstadt, Germany

Z. Naturforsch. **47a**, 689–701 (1992); received January 16, 1992

The molecular dynamics of tetramethylstibonium hexafluorophosphate, $[\text{Sb}(\text{CH}_3)_4]\text{PF}_6$, is investigated over a broad temperature range. NMR spin lattice relaxation times T_1 and the NMR second moments of the ^1H and ^{19}F nuclei were determined in the range $8.6 \leq T/\text{K} \leq 332.3$ for polycrystalline $[\text{Sb}(\text{CH}_3)_4]\text{PF}_6$. The complex cation undergoes isotropic tumbling for $T > 260$ K and thermally activated methyl group rotation in the temperature range $T < 196$ K. The activation energies for the transition from methyl group rotation to cation reorientation, as derived from NMR wideline (18.1 kJ/mol) and relaxation (22.7 kJ/mol) measurements, match. At very low temperatures pseudo classical line narrowing is observed, indicating tunneling motions of the methyl groups. The existence of two crystallographically inequivalent methyl groups is found by X-ray structure analysis at room temperature. The space group is $\text{P}6_3\text{mc}$, $Z=2$; $a=738.6$ pm, $c=1089.3$ pm. It is confirmed by two steps in the temperature dependence of the signal intensity of the quasielastic line in neutron fixed window measurements in the temperature range $2 < T/\text{K} < 148$. The low temperature spin lattice relaxation times can be explained qualitatively by contributions of two crystallographically inequivalent methyl groups. Apparent activation energies for the two crystallographically different methyl groups are estimated.

The complex anion undergoes isotropic tumbling in the temperature range $95 < T/\text{K} < 330$. Above 330 K additionally translational motion is activated. Below 95 K the rotational motion of PF_6^\ominus is freezing in via an uniaxial state in range $40 < T/\text{K} < 80$. Activation energies for both isotropical tumbling (10.5 kJ/mol) and uniaxial rotation (5.8 kJ/mol) have been derived from ^{19}F NMR spin lattice relaxation.

Key words: Complex compounds, Molecular dynamics, Rotational tunneling, Nuclear magnetic resonance spectroscopy, Quasielastic neutron scattering.

Introduction

Solids containing the highly symmetric species $\text{X}(\text{CH}_3)_4$ show several degrees of molecular motion. At high temperatures thermally activated overall tumbling as well as methyl group rotation about the three-fold symmetry axes can be detected and described classically. At very low temperatures quantum mechanical tunneling of the methyl groups may dominate if the rotational barrier of the methyl groups is low and the classical approaches are not adequate to explain the results. This was found e.g. for molecular $\text{Sn}(\text{CH}_3)_4$ [1, 2] and ionic $[\text{Sb}(\text{CH}_3)_4]\text{I}$ [3, 4].

In combination with complex anions containing nuclei with a considerable magnetic moment (BF_4^\ominus , PF_6^\ominus), both independent and coupled relaxation of cationic and anionic spin systems can occur [5, 6]. Using nuclear magnetic resonance (NMR), second moment (M_2) and spin lattice relaxation time (T_1) techniques, cationic and anionic motions can be resolved and motional parameters derived.

Only few investigations are known where an analysis of the rotational behaviour by means of second moments and relaxation times has been executed from the limit very high temperatures to liquid helium temperatures [7, 8].

The present study was undertaken to determine the molecular dynamics of tetramethylstibonium hexafluorophosphate, $[\text{Sb}(\text{CH}_3)_4]^\oplus\text{PF}_6^\ominus$, over a broad temperature range and to compare the cationic dynamics with those of tetramethylstibonium iodide, $[\text{Sb}(\text{CH}_3)_4]^\oplus\text{I}^\ominus$, where a large activation energy for

* Part of Dr.-Ing. thesis of Günter Burbach, TH Darmstadt (D17).

Reprint requests to Prof. Dr. Al. Weiss, Institut für Physikalische Chemie, Technische Hochschule Darmstadt, Petersenstraße 20, W-6100 Darmstadt.

0932-0784 / 92 / 0500-0689 \$ 01.30/0. – Please order a reprint rather than making your own copy.



Dieses Werk wurde im Jahr 2013 vom Verlag Zeitschrift für Naturforschung in Zusammenarbeit mit der Max-Planck-Gesellschaft zur Förderung der Wissenschaften e.V. digitalisiert und unter folgender Lizenz veröffentlicht: Creative Commons Namensnennung-Keine Bearbeitung 3.0 Deutschland Lizenz.

Zum 01.01.2015 ist eine Anpassung der Lizenzbedingungen (Entfall der Creative Commons Lizenzbedingung „Keine Bearbeitung“) beabsichtigt, um eine Nachnutzung auch im Rahmen zukünftiger wissenschaftlicher Nutzungsformen zu ermöglichen.

This work has been digitalized and published in 2013 by Verlag Zeitschrift für Naturforschung in cooperation with the Max Planck Society for the Advancement of Science under a Creative Commons Attribution-NoDerivs 3.0 Germany License.

On 01.01.2015 it is planned to change the License Conditions (the removal of the Creative Commons License condition "no derivative works"). This is to allow reuse in the area of future scientific usage.

the transition from methyl group rotation to overall cation tumbling was found. Rotational tunneling of the methyl groups in $[\text{Sb}(\text{CH}_3)_4]\text{I}$ was manifested by $M_2(^1\text{H})$, $T_1^{-1}(^1\text{H})$, and inelastic neutron scattering [4].

The activation energy for isotropical PF_6^\ominus reorientation has been determined for a series of alkali hexafluorophosphates APF_6 , $\text{A} = \text{Na}, \text{K}, \text{Rb}, \text{Cs}$, and found to depend on the cation size [9]. Substituting the $\text{Sb}(\text{CH}_3)_4^\oplus$ cation, this correlation can be proved.

Experimental

T_1 Measurements

Proton and fluorine spin lattice relaxation times $T_1(^1\text{H})$ and $T_1(^{19}\text{F})$, respectively, of tetramethylstibonium hexafluorophosphate, $[\text{Sb}(\text{CH}_3)_4]\text{PF}_6$, prepared as described in a previous paper [3], were measured at two different Larmor frequencies $\omega_0/2\pi = 21.02$ MHz and $\omega_0/2\pi = 36.55$ MHz. A temperature range $8.6 \leq T/\text{K} \leq 332.3$ was covered. Temperatures were controlled by a continuous flow cryostat. For $T > 73$ K liquid nitrogen and for $T < 73$ K liquid helium was used as coolant. At a given temperature the sample was equilibrated thermally for at least 15 min. A copper-constantan thermocouple (N_2 cooling) and a NiCr–Au 0.02 atom% Fe thermocouple (He cooling), respectively, were employed to monitor the temperature near the sample site. The polycrystalline sample was sealed in a glass ampoule under helium as heat exchange gas. Spin lattice relaxation times were measured by means of $180^\circ - \tau - 90^\circ$ pulse sequences and determined by an exponential fitting procedure [10]. Errors of the T_1 values measured are estimated to be $\pm 5\%$, while those in the temperature measurements are ± 0.2 K.

Wideline Measurements

Proton and fluorine NMR second moments $M_2(^1\text{H})$ and $M_2(^{19}\text{F})$, respectively, have been measured down to 8 K using a modified Robinson-oscillator [11] operating at a constant frequency of 28.55 MHz by slowly varying the magnetic induction B_0 . Spectra of polycrystalline specimen were recorded by lock-in technique. The line widths ΔB were taken as separation in Tesla between the extrema of the derivative curves. M_2 values were calculated using a numerical integration procedure. Correction due to finite field modulation broadening was considered

[12]. Temperatures were controlled by a continuous flow liquid He cryostat and measured near the sample site with a NiCr–Au 0.02 atom% Fe thermocouple. The sample was thermally equilibrated at least for 10 min at a given temperature. The variation of the temperature during the data acquisition was ± 0.5 K.

Fixed Window Measurements

Quasielastic neutron scattering (QNS) experiments were carried out at the Institute Laue-Langevin (ILL), Grenoble, using the backscattering spectrometer IN10. Identical material as in the NMR experiments was used. The IN10 spectrometer was set to zero energy transfer and the intensity of the elastic line was measured in the temperature interval $2.5 \leq T/\text{K} \leq 147$ ('fixed window scan') with an energy resolution $\delta E_{\text{res}} = 0.5 \mu\text{eV}$.

Results

^1H and ^{19}F NMR Spin Lattice Relaxation Times

The experimental proton and fluorine spin lattice relaxation rates $1/T_1$ of polycrystalline $[\text{Sb}(\text{CH}_3)_4]\text{PF}_6$ observed at 21.02 MHz and 36.55 MHz, respectively, are shown in Fig. 1–4 as semilogarithm plots versus inverse temperature.

The spin lattice relaxation rates of the fluorine nuclei parallel those for protons over a wide temperature range. Within the interval $35 < T/\text{K} < 40$ nonexponential relaxation was observed. The deviation from single exponential relaxation was small and all relaxation times have been described by a single relaxation time $T_1(^{19}\text{F})$ and $T_1(^1\text{H})$, respectively, within the limits of error.

The spin lattice relaxation times of the protons (Figs. 1 and 2) are always higher than the fluorine relaxation times (Figs. 3 and 4), except in the limits of very high and very low temperatures (i.e. for $T > 277$ K and $T < 34$ K at 36.55 MHz, respectively), where $T_1(^1\text{H})$ becomes shorter than $T_1(^{19}\text{F})$.

The proton relaxation rates $1/T_1(^1\text{H}) = f(T)$ show four and the fluorine relaxation rates $1/T_1(^{19}\text{F}) = f(T)$ three maxima. The maximum on the high temperature side is higher for $1/T_1(^1\text{H})$ and located at a higher temperature (see Fig. 1) than the maximum of $1/T_1(^{19}\text{F})$, Figure 3.

In the intermediate temperature range the relaxation curves show a broad maximum at 145 K for

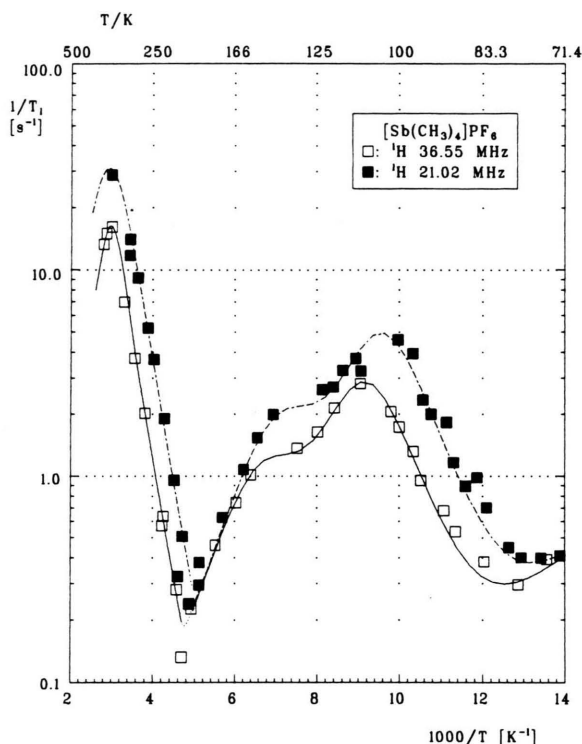


Fig. 1. Proton spin lattice relaxation rates $1/T_1(^1\text{H})$ of tetramethylstibonium hexafluorophosphate, $[\text{Sb}(\text{CH}_3)_4]\text{PF}_6$, as function of the inverse temperature in the range $2.4 \leq 1000 \text{ K}/T \leq 14$. Open and filled symbols represent $1/T_1(^1\text{H})$ at the two Larmor frequencies $\omega_0/2\pi = 36.55 \text{ MHz}$ and $\omega_0/2\pi = 21.02 \text{ MHz}$, respectively. The lines correspond to the theoretical description given in the text.

$1/T_1(^{19}\text{F})$ and 112 K for $1/T_1(^1\text{H})$ (Figs. 1 and 3). At very low temperatures a $1/T_1(^{19}\text{F})$ maximum at 45 K is observed, whereas for $1/T_1(^1\text{H})$ two maxima are found, a large one at $T = 39 \text{ K}$ and a very broad one at $T \approx 10 \text{ K}$. The maxima for both, ^1H and ^{19}F nuclei are frequency dependent.

^1H and ^{19}F NMR Second Moments

To attribute the various maxima in the $1/T_1$ relaxation curves of the protons and fluorine nuclei to any molecular/ionic motion in $[\text{Sb}(\text{CH}_3)_4]\text{PF}_6$, the second moments $M_2(^{19}\text{F})$ and $M_2(^1\text{H})$ were measured for $T < 95 \text{ K}$ and for $T > 330 \text{ K}$. The experimental results are shown in Figs. 5 and 6 together with the values given previously for $95 < T/\text{K} < 330$ [3].

For $T > 325 \text{ K}$ $M_2(^{19}\text{F})$ decreases from $0.6 \times 10^{-8} \text{ T}^2$ to $0.3 \times 10^{-8} \text{ T}^2$ (see Figure 6). The step in $M_2(^1\text{H})$ at $T = 325 \text{ K}$ is less pronounced. Below 120 K

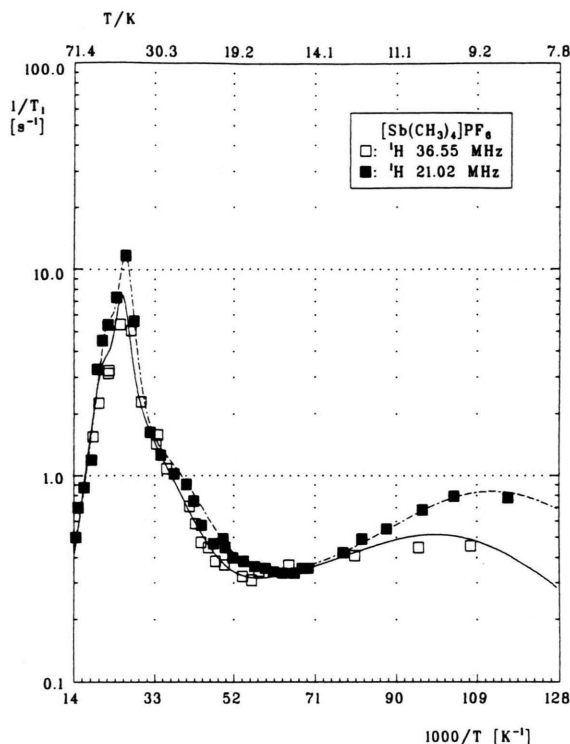


Fig. 2. Same as Figure 1 but for the temperature range $14 \leq 1000 \text{ K}/T \leq 128$.

$M_2(^{19}\text{F})$ raises with constant but a less steep slope in the range $40 < T/\text{K} < 70$. At the lowest temperature reached experimentally, $M_2(^{19}\text{F})$ attains its maximal value $M_2(7.6 \text{ K}) = 11.4 \times 10^{-8} \text{ T}^2$.

In contrast to $M_2(^{19}\text{F})$, the linewidth $\Delta B(^{19}\text{F})$ does not show any sign of a plateau in the range $40 < T/\text{K} < 70$ (see Figure 5). By further decreasing the temperature to 30 K, $\Delta B(^{19}\text{F})$ increases only slowly, and for $T < 30 \text{ K}$ it increases strongly to a maximum value at $T = 7.6 \text{ K}$ (see Figure 6). The line shape of the ^{19}F resonance signal changes drastically. In Fig. 7 the derivative absorption curves at various temperatures are given. An asymmetry of the curves due to chemical shift anisotropy, as observed for the ^{19}F line shape of NH_4PF_6 [13], was not observed. For temperatures $T > 130 \text{ K}$ the signal can be described by a single Gaussian curve. On decreasing the temperature, the wings of the absorption line gain intensity (cf. Fig. 7 for $T = 77.1 \text{ K}$ and $T = 60.1 \text{ K}$). At $T = 30.4 \text{ K}$ a second, broad component with an intensity equal to the center line arises, and at $T = 7.6 \text{ K}$ the center line is vanished completely. The whole intensity is transferred into the outer component. The jump-like step in

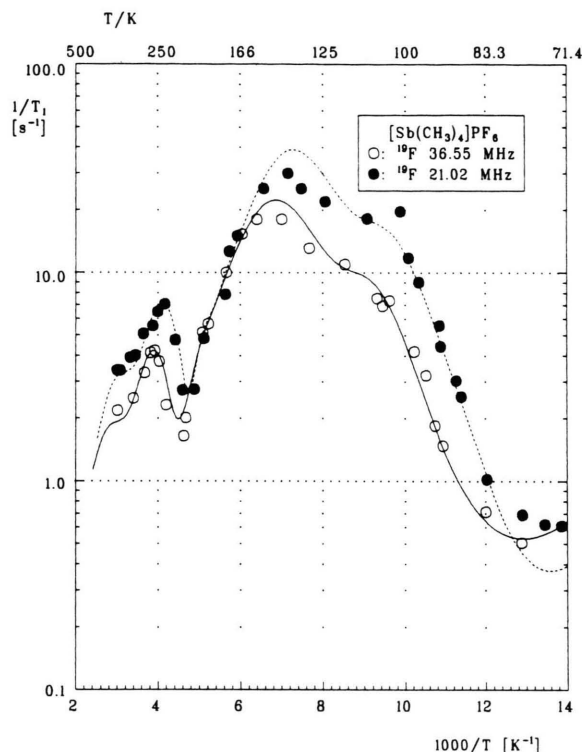


Fig. 3. Fluorine spin lattice relaxation rates $1/T_1(^{19}\text{F})$ of tetramethylstibonium hexafluorophosphate, $[\text{Sb}(\text{CH}_3)_4]\text{PF}_6$, as function of the inverse temperature in the range $2.4 \leq 1000 \text{ K}/T \leq 14$. Open and filled symbols represent $1/T_1(^{19}\text{F})$ at the two Larmor frequencies $\omega_0/2\pi = 36.55 \text{ MHz}$ and $\omega_0/2\pi = 21.02 \text{ MHz}$, respectively. The lines correspond to the theoretical description given in the text.

the $\Delta B(^{19}\text{F})$ vs. T diagram (see Fig. 6) is due to the transition in maximum intensity from the narrow vanishing to the broad growing component.

At lowest temperatures a constant plateau has not been reached neither in $M_2(^{19}\text{F})$ nor in $\Delta B(^{19}\text{F})$.

Both, $M_2(^1\text{H})$ and $\Delta B(^1\text{H})$ show a small step around $T \approx 100 \text{ K}$. The $M_2(^1\text{H})$ plateau increases from $7.8 \times 10^{-8} \text{ T}^2$ to $8.5 \times 10^{-8} \text{ T}^2$ for $T < 120 \text{ K}$ (see Figure 5). As can be seen from Fig. 8, there is no significant change in line shapes of the proton resonance signals for $T < 190 \text{ K}$. At the high temperature limit a further decrease of $M_2(^1\text{H})$ from $0.6 \times 10^{-8} \text{ T}^2$ to $0.5 \times 10^{-8} \text{ T}^2$ at 325 K is observed.

Fixed Window Measurements

The intensities of the fixed window scans of tetramethylstibonium hexafluorophosphate as obtained at a detector angle $2\theta = 130^\circ$ are shown in Figure 9. Two

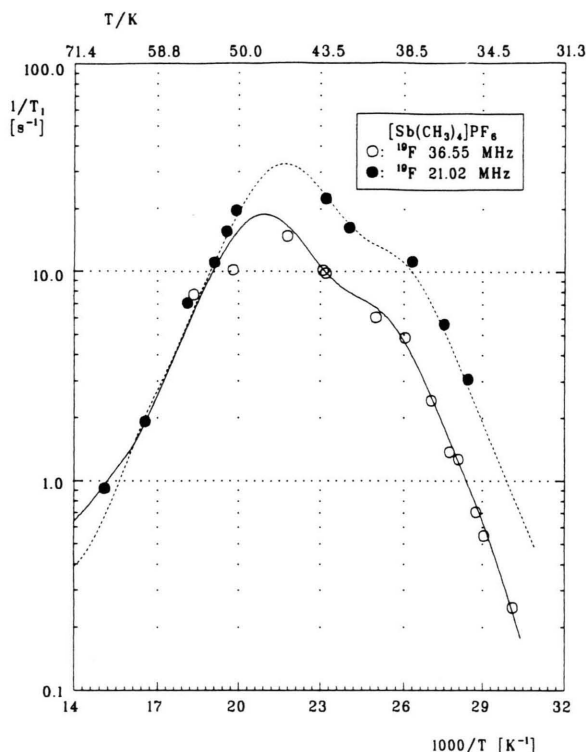


Fig. 4. Same as Fig. 3 but for the temperature range $14 \leq 1000 \text{ K}/T \leq 32$.

steps at $T = 17.0 \text{ K}$ and $T = 46.0 \text{ K}$ were found. They can be attributed to jumps of two crystallographically inequivalent methyl groups across the rotational barrier [4, 14]. The temperature dependence of the quasi-elastic line width Γ_{qu} can be described by an Arrhenius Ansatz

$$\Gamma_{\text{qu}}(T) = \Gamma_0 \exp(-E_a/RT). \quad (1)$$

Γ_0 is connected with correlation time constants as obtained from the high temperature side of the relaxation curves [14]. At that temperature $T_{1/2}$, where half of the height of the quasielastic line is transferred out of the elastic energy window, the condition $\Gamma_{\text{qu}} = \delta E_{\text{res}}$ is valid and the barrier height given by [2]

$$E_a = R \ln(\Gamma_0/\delta E_{\text{res}}) T_{1/2}. \quad (2)$$

Discussion

Determination of the Motional States

For tetramethylstibonium hexafluorophosphate the temperature dependence of $M_2(^1\text{H})$ and $M_2(^{19}\text{F})$ in

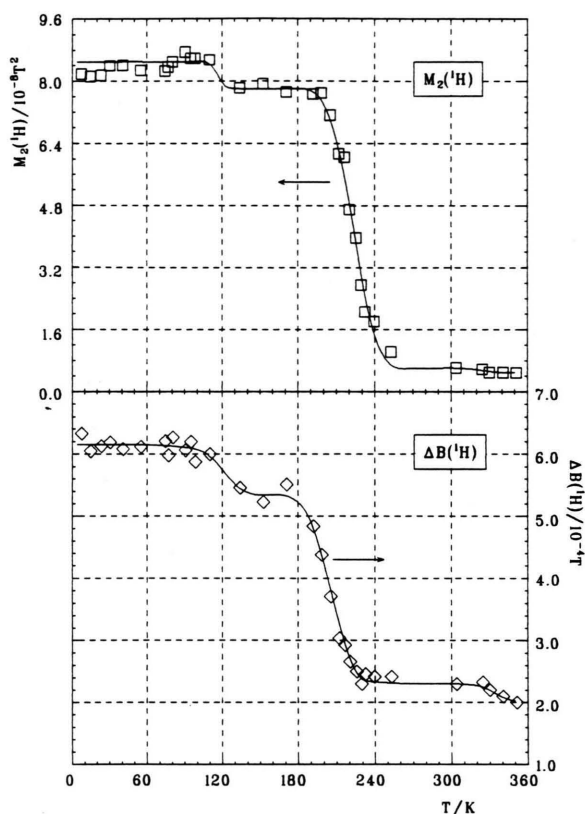


Fig. 5. Second moment $M_2(\square)$ and linewidth $\Delta B(\diamond)$ of the proton NMR signal of tetramethylstibonium hexafluorophosphate at constant Larmor frequencies $\omega_0/2\pi = 28.55$ MHz and $\omega_0/2\pi = 8.10$ MHz ($96 \leq T/\text{K} \leq 324$), respectively, as function of temperature. Values at 8.10 MHz were taken from [3]. (Lines serve as guide for the eye.)

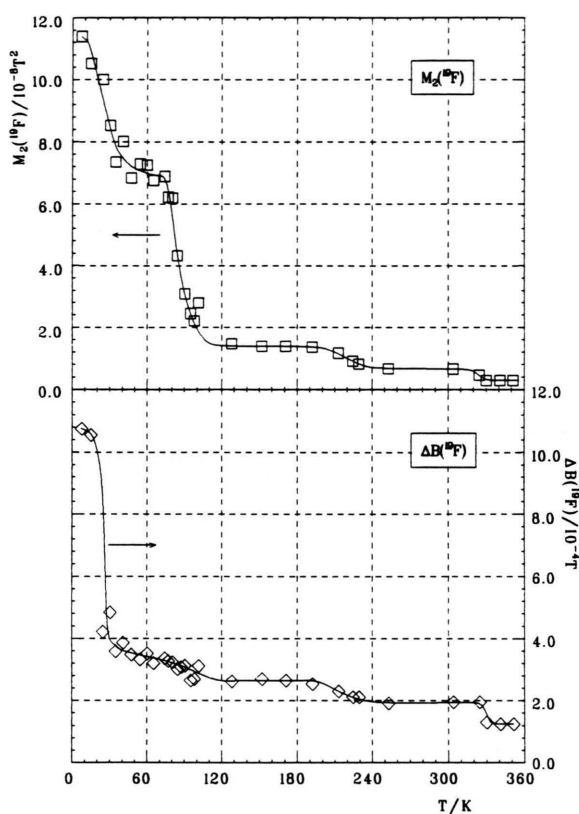


Fig. 6. Second moment $M_2(\square)$ and linewidth $\Delta B(\diamond)$ of the fluorine NMR signal of tetramethylstibonium hexafluorophosphate at constant Larmor frequencies $\omega_0/2\pi = 28.55$ MHz and $\omega_0/2\pi = 8.10$ MHz ($96 \leq T/\text{K} \leq 324$), respectively, as function of temperature. Values at 8.10 MHz were taken from [3]. (Lines serve as guide for the eye.)

the range $96 \leq T/\text{K} \leq 324$ has been measured previously [3]. A change in the motional state of $[\text{Sb}(\text{CH}_3)_4]\text{PF}_6$ has been found. It was attributed to the freezing-in process of the isotropic $[\text{Sb}(\text{CH}_3)_4]^+$ cation tumbling in the range $196 \leq T/\text{K} \leq 260$, which leads to an increase of $M_2(^1\text{H})$ from $0.6 \times 10^{-8} \text{ T}^2$ for $T > 260 \text{ K}$ to $7.8 \times 10^{-8} \text{ T}^2$ for $T < 196 \text{ K}$.

$M_2(^{19}\text{F})$ is influenced via H–F dipolar interactions and reflects the transition in the cation motion by a small step from $0.6 \times 10^{-8} \text{ T}^2$ to $1.4 \times 10^{-8} \text{ T}^2$ in the same temperature region, $196 \leq T/\text{K} \leq 260$. The complex anion PF_6^- reorients isotropically over the whole temperature range $95 < T/\text{K} < 330$. Reorientations about unique axes (two-, three-, and fourfold symmetry axes) can be excluded. The second moments calculated on the base of crystal structure data are consistent with the values observed experimentally [3].

Combining the results of the ^1H and ^{19}F NMR wideline measurements of tetramethylstibonium hexafluorophosphate found in this study, the following picture is obtained:

In the high temperature limit of the temperature range investigated, the $[\text{Sb}(\text{CH}_3)_4]^+$ cations and the PF_6^- anions perform isotropic reorientations about random axes with simultaneous rotation of the methyl groups about their threefold (C_3) axes in the cation.

The decrease of the second moments $M_2(^{19}\text{F})$ and $M_2(^1\text{H})$ for $T > 330 \text{ K}$ is due to the onset of additional motion. Since all degrees of rotational freedom are excited, we assume that translational motion sets in. Because the change in $M_2(^{19}\text{F})$ from $0.6 \times 10^{-8} \text{ T}^2$ to $0.3 \times 10^{-8} \text{ T}^2$ is larger than the one in $M_2(^1\text{H})$ from $0.6 \times 10^{-8} \text{ T}^2$ to $0.5 \times 10^{-8} \text{ T}^2$, the steps must be caused by translational diffusion of the PF_6^- anions.

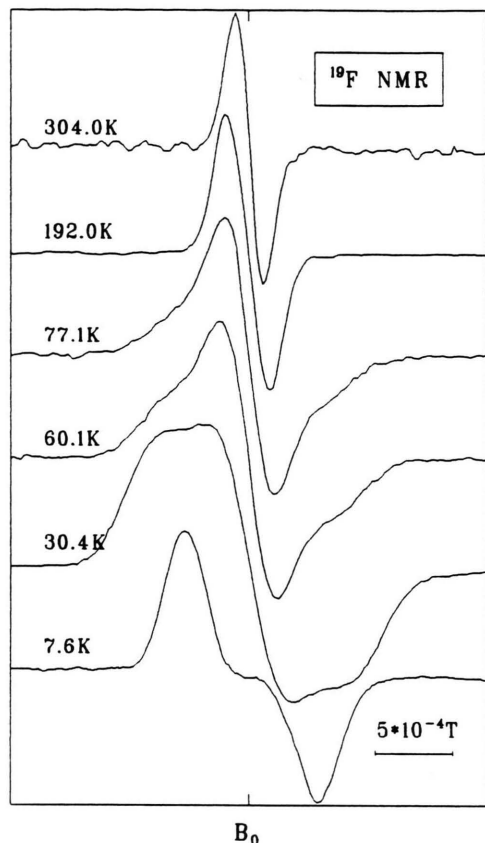


Fig. 7. Derivative absorption curves of the ^{19}F NMR resonance of $[\text{Sb}(\text{CH}_3)_4]\text{PF}_6$ at selected temperatures. The signal amplitudes are normalised to unity ($B_0 = 0.21$ T).

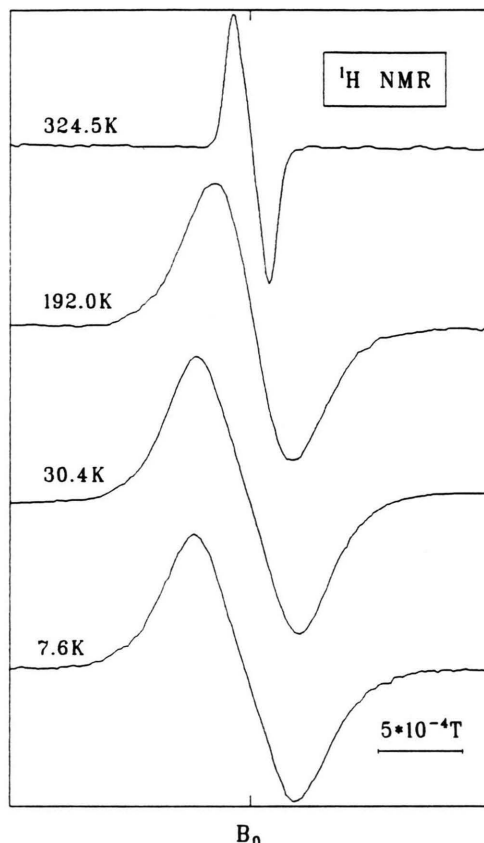


Fig. 8. Derivative absorption curves of the ^1H NMR resonance of $[\text{Sb}(\text{CH}_3)_4]\text{PF}_6$ at various temperatures. The signal amplitudes are normalised to unity ($B_0 = 0.19$ T).

An onset of diffusion of the cations would have a large effect on $M_2(^1\text{H})$ and a small influence on $M_2(^{19}\text{F})$ since 12 protons and only 6 fluorine nuclei would be involved and the H–F dipolar interactions are smaller than the H–H dipolar interactions. Thus, cation diffusion can be excluded.

Not only from the value of $M_2(^1\text{H})$, but also from the line shape of the proton resonance signal at the limit of very low temperatures it can be seen that the rotational motions of the methyl groups are not frozen in (see Figs. 5 and 8). The M_2 value of an isolated rigid methyl group, neglecting dipolar inter- and intramolecular/-ionic interactions, is $21.3 \times 10^{-8} \text{ T}^2$ and by no means reached by $[\text{Sb}(\text{CH}_3)_4]^+\text{PF}_6^-$. The small change in $M_2(^1\text{H})$ at $T \approx 10$ K, which can also be seen in $\Delta B(^1\text{H})$, must be caused mainly by a change of the rotational motion of the PF_6^- anion.

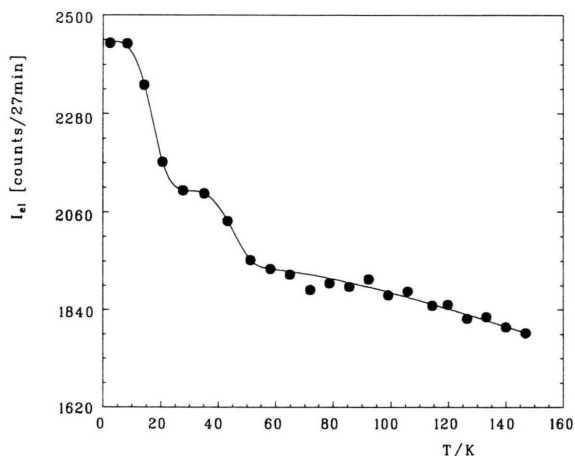


Fig. 9. Fixed window measurement of the elastic scattering from tetramethylstibonium hexafluorophosphate, $[\text{Sb}(\text{CH}_3)_4]\text{PF}_6$, at a momentum transfer $Q = 1.94 \text{ \AA}^{-1}$.

As can be seen from $M_2(^{19}\text{F})$ and the line shape of the resonance signal of the fluorine nuclei at $T = 7.6$ K (see Figs. 6 and 7), the rotational motion of PF_6^\ominus is freezing in at the low temperature limit. The value for the second moment of an isolated rigid regular PF_6^\ominus octahedron with a P–F bond length of 158 pm is given by $M_2(\text{F–F}) = 10.52 \times 10^{-8} \text{ T}^2$ plus $M_2(\text{F–P}) = 1.68 \times 10^{-8} \text{ T}^2$ [3], the sum for which being in good agreement with $M_2(^{19}\text{F}) = 11.4 \times 10^{-8} \text{ T}^2$ observed experimentally at 7.6 K. The plateau of ca. $7 \times 10^{-8} \text{ T}^2$ in the narrow temperature range $40 \leq T/\text{K} \leq 70$ indicates that the transition from isotropic tumbling to stationary PF_6^\ominus anions must be connected with rotation about an unique axis. Since the intermolecular $M_2(^{19}\text{F})$ contributions are not expected to change these ratios grossly and the difference between the experimental value and the calculated one is largest for fourfold reorientations, it may be assumed that in the range $40 \leq T/\text{K} \leq 70$ the PF_6^\ominus anions undergo two- or threefold reorientations before any motion is freezing in. A clear decision about the symmetry axis on the base of M_2 measurements can not be done.

Previously we reported single crystal X-ray diffraction studies of some tetramethylstibonium compounds at room temperature [3]. For tetramethylstibonium hexafluorophosphate definitive positions of the atoms of the anion could not be determined because of difficulties in locating the phosphorus atom. Nevertheless, the preliminary crystallographic data and relative atomic coordinates concerning the $[\text{Sb}(\text{CH}_3)_4]^\oplus$ cation shall be communicated here. As will be seen below, results of the determination of the cation geometry can be discussed in connection with low temperature ^1H NMR spin lattice relaxation and quasielastic scattering data. From the diffraction extinctions the space groups $\text{P}6_3\text{mc}$, $\text{P}6_2\text{c}$, and $\text{P}6_3/\text{mmc}$ can be deduced. The direct method (Shelx86) was used to determine the positions of antimony. The carbon sites were obtained from difference-Fourier-syntheses. P, F, and H positions could not be located.

In Tables 1 and 2 the experimental conditions for the crystal structure determination and the relative atomic coordinates of the carbon and antimony atoms based upon the space group $\text{P}6_3\text{mc}$ with $Z=2$ formula units per unit cell are given. In Table 3 intra- and some inter- $\text{Sb}(\text{CH}_3)_4^\oplus$ distances and angles are listed.

The cation consists of a distorted $[\text{Sb}(\text{CH}_3)_4]^\oplus$ tetrahedron with four methyl groups in the corners and the Sb in the center. Two crystallographic inequivalent carbon atoms $\text{C}^{(1)}$ and $\text{C}^{(2)}$ in the ratio 3:1 were

Table 1. Experimental conditions for the crystal structure determination of tetramethylstibonium hexafluorophosphate at $T=301$ K and crystallographic data.

Formula unit	$[\text{Sb}(\text{CH}_3)_4]\text{PF}_6$
Crystal habitus	6-sided prism, colourless
Crystal size/mm ³	$0.22 \times 0.28 \times 2.00$
Formula weight/g/mol	326.85
Diffractionmeter	Stoe-Stadi-4
Wavelength λ/pm	71.069 (MoK α)
Monochromator	graphite (002)
Absorption coefficient μ/m^{-1}	2890
Scan	$\omega/2\theta$
$(\sin \theta/\lambda)_{\text{max}}/\text{pm}^{-1}$	0.0068
Number of measured reflexions	3969
Symmetry independent reflexions	750
Reflexions considered	500
Free parameters	19
$F(000)$	266
$R(\text{F})$	0.0710
$R_w(\text{F})$	0.0620
Lattice constants:	
a/pm	738.6 (2)
c/pm	1089.3 (3)
Volume of the unit cell	
$V \times 10^{-6}/(\text{pm})^3$	514.66 (42)
Probable space group	$\text{C}_{6v}^4 - \text{P}6_3\text{mc}$
Formula units per unit cell	$Z=2$
$\rho_{\text{calc}}/\text{Mgm}^{-3}$	2.109 ($T=301$ K)
$\rho_{\text{pykn}}/\text{Mgm}^{-3}$	2.09 ($T=295$ K)
Point positions	
$\text{C}^{(1)}$ in 6c:	$x, \bar{x}, z; x, 2x, z;$ $2\bar{x}, \bar{x}, z; \bar{x}, x, 1/2+z;$ $\bar{x}, 2\bar{x}, 1/2+z; 2x, x, 1/2+z$
Sb and $\text{C}^{(2)}$ in 2b:	$1/3, 2/3, z; 2/3, 1/3, 1/2+z$

found. As it is the case in tetramethylstibonium iodide, space group $\text{P}6_3\text{mc}$, the Sb–C bond length to the unique $\text{C}^{(2)}$ atom is greater than to $\text{C}^{(1)}$. In $[\text{Sb}(\text{CH}_3)_4]\text{I}$ $d(\text{Sb–C}^{(1)}) = 208.1$ pm, $d(\text{Sb–C}^{(2)}) = 211.5$ pm [3], whereas in $[\text{Sb}(\text{CH}_3)_4]\text{PF}_6$ $d(\text{Sb–C}^{(1)}) = 206.0$ pm, $d(\text{Sb–C}^{(2)}) = 215.6$ pm (in this work the superscript 1 of a carbon atom or index 1 of a methyl group denote the more frequently occurring crystallographically inequivalent C or CH_3 , respectively).

The ratio of the axes of a hexagonal unit cell is a measure for the deviation from dense packing of spheres. For $[\text{Sb}(\text{CH}_3)_4]\text{PF}_6$ $c/a = 1.475$, which is only little greater than 1.425 found for $[\text{Sb}(\text{CH}_3)_4]\text{I}$ but smaller than the ideal ratio for a hexagonal closest packing of spheres (1.633) [3].

The Sb–C bond length weighted by the ratio of occurrence, $d\langle\text{Sb–C}\rangle = 208.4$ pm, for $[\text{Sb}(\text{CH}_3)_4]\text{PF}_6$ is short in comparison with mean bond lengths of other methylated Sb compounds [15, 16].

From the ^1H and ^{19}F NMR second moment measurements it is not unreasonable that the determina-

Table 2. Positional and thermal parameters of $\text{Sb}(\text{CH}_3)_4^\oplus$ cation in tetramethylstibonium hexafluorophosphate as obtained from a single crystal X-ray structure determination at $T = 301$ K. The temperature factor is of the form $T = \exp(-2\pi^2(U_{11}h^2a^{*2} + U_{22}k^2b^{*2} + U_{33}l^2c^{*2} + 2U_{12}hka^*b^* + 2U_{13}hla^*c^* + 2U_{23}klb^*c^*))$. The U_{ij} are given in $(\text{pm})^2$; errors are given in brackets (U is the isotropic mean).

Atom	x/a	y/b	z/c	U_{11}, U	U_{22}	U_{33}	U_{12}	U_{13}	U_{23}
Sb	0.3333 (0)	0.6667 (0)	0 (0)	532 (40)	527 (52)	936 (12)	0 (0)	155 (30)	0 (0)
C ⁽¹⁾	0.1789 (13)	0.8211 (13)	0.0533 (14)	1238 (56)					
C ⁽²⁾	0.3333 (0)	0.6667 (0)	0.3021 (28)	1292 (102)					

Table 3. Intra- and short inter- $\text{Sb}(\text{CH}_3)_4^\oplus$ bond distances and bond angles of tetramethylstibonium hexafluorophosphate. Errors and abundance of equal atoms are given in brackets, respectively.

Intra- $\text{Sb}(\text{CH}_3)_4^\oplus$	Distance/pm
Sb–C ⁽¹⁾	206.0 (9) ($3 \times$)
Sb–C ⁽²⁾	215.6 (16) ($1 \times$)
C ⁽¹⁾ ... C ⁽²⁾	337.5
C ⁽¹⁾ ... C ⁽¹⁾	342.2
Inter- $\text{Sb}(\text{CH}_3)_4^\oplus$	Distance/pm
Sb ... Sb	691.7
C ⁽¹⁾ ... C ⁽¹⁾	396.6
C ⁽²⁾ ... C ⁽¹⁾	458.4
C ⁽²⁾ ... C ⁽²⁾	691.7
(A–B–C)	Angle/degree
C ⁽¹⁾ –Sb–C ⁽²⁾	106.4 (2)
C ⁽¹⁾ –Sb–C ⁽¹⁾	112.4 (2)

tion of the PF_6^\ominus structural data failed. The crystal structure determination has been executed at 301 K, where the onset of translational motion of the PF_6^\ominus ions may already be activated. Since at room temperature all rotational degrees of freedom are acti-

described by a pair of coupled differential equations [18],

$$\begin{aligned} dM_z(\text{H})/dt = & -T_1^{-1}(\text{HH})[\langle M_z(\text{H}) \rangle - M_0(\text{H})] \\ & -T_1^{-1}(\text{HF})[\langle M_z(\text{F}) \rangle - M_0(\text{F})] \end{aligned} \quad (3)$$

and

$$\begin{aligned} dM_z(\text{F})/dt = & -T_1^{-1}(\text{FH})[\langle M_z(\text{H}) \rangle - M_0(\text{H})] \\ & -T_1^{-1}(\text{FF})[\langle M_z(\text{F}) \rangle - M_0(\text{F})], \end{aligned} \quad (4)$$

where the quantities $\langle M_z(\text{H}) \rangle$, $\langle M_z(\text{F}) \rangle$ and $M_0(\text{H})$, $M_0(\text{F})$ are the components of the proton and fluorine nuclear magnetizations in the direction of \mathbf{B}_0 at time t and at thermal equilibrium, respectively. $T_1^{-1}(\text{HH})$, $T_1^{-1}(\text{FF})$, $T_1^{-1}(\text{FH})$, and $T_1^{-1}(\text{HF})$ are the elements of the relaxation matrix.

The relaxation times are given by

$$\frac{M_0(\text{H}) - \langle M_z(\text{H}) \rangle}{2M_0(\text{H})} = A \exp(-\lambda_1 t) + B \exp(-\lambda_2 t). \quad (5)$$

The same expression with H replaced by F and reversed λ_1 and λ_2 applies to the fluorine nuclei [13]. A and B represent relaxation constants and λ_1 and λ_2 are eigenvalues of the relaxation matrix:

$$\begin{aligned} \lambda_{1,2} = & \frac{1}{2}(T_1^{-1}(\text{HH}) + T_1^{-1}(\text{FF})) \\ & \pm \frac{1}{2}\sqrt{(T_1^{-1}(\text{HH}) + T_1^{-1}(\text{FF}))^2 - 4T_1^{-1}(\text{HH})T_1^{-1}(\text{FF}) + 4T_1^{-1}(\text{FH})T_1^{-1}(\text{HF})}. \end{aligned} \quad (6)$$

vated and anion diffusion sets in, the state of $[\text{Sb}(\text{CH}_3)_4]^\oplus\text{PF}_6^\ominus$ can be described as a quasi plastic crystal [17] and therefore a structure determination should be promising at lower temperatures ($T < 200$ K, see Fig. 5) and with deuterated methyl groups, if statements about H sites are required.

Reorientational Motion at High Temperatures

The NMR spin lattice relaxation mechanism of compounds containing ^1H and ^{19}F spin system can be

Two limiting cases can be distinguished. If one of the diagonal matrix elements $T_1^{-1}(\text{HH})$ or $T_1^{-1}(\text{FF})$, respectively, predominates over the rest, the variation of the longitudinal magnetization of the respective relaxation rate only is observable and single exponential relaxation would be observed. In this case it is not necessary to evaluate $T_1^{-1}(\text{FH})$ and $T_1^{-1}(\text{HF})$.

If, on the other hand, all elements of the relaxation matrix are of the same order of magnitude, cross relaxation between the ^1H and ^{19}F nuclei must be considered and nonexponential relaxation behaviour is expected.

Because the quadrupole moments of the ^{121,123}Sb nuclei are quite high it is assumed that the quadrupole coupling of these nuclei is strong enough to maintain the Sb spin system in thermal equilibrium with the lattice.

Since single exponential relaxation was observed nearly in the whole temperature range studied, the relaxation rates are given by the equations consisting of the spectral density functions $g(\omega, \tau)$ as [13]

$$\begin{aligned} \frac{1}{T_1(^1\text{H})} = & \frac{2}{3} \gamma_{\text{H}}^2 \Delta M_2(\text{HH}) g(\omega_{\text{H}}, \tau_{\text{H}}) \\ & + \frac{1}{2} \gamma_{\text{H}}^2 \Delta M_2(\text{HF}) g(\omega_{\text{H}}, \omega_{\text{F}}, \tau_{\text{H}}) \\ & + \frac{1}{2} \gamma_{\text{H}}^2 \Delta M_2(\text{HP}) g(\omega_{\text{H}}, \omega_{\text{P}}, \tau_{\text{H}}) \quad (7) \end{aligned}$$

$$\frac{1}{T_1(^{19}\text{F})} = \frac{1}{2} \gamma_{\text{H}}^2 \Delta M_2(\text{FH}) g(\omega_{\text{F}}, \omega_{\text{H}}, \tau_{\text{F}}). \quad (8)$$

$\Delta M_2(\text{IS})$ is the reduction of the second moment of the I spins ($M_2(\text{I})$) due to magnetic dipolar interactions with the spins S, which is modulated by the respective ionic motion; ω_{H} , ω_{F} , and ω_{P} are the Larmor frequencies of the ¹H, ¹⁹F, and ³¹P nuclei, respectively, and γ denotes the magnetogyric constant.

The spectral density functions are given as

$$g(\omega_{\text{I}}, \tau_{\text{I}}) = \frac{\tau_{\text{I}}}{1 + \omega_{\text{I}}^2 \tau_{\text{I}}^2} + \frac{4 \tau_{\text{I}}}{1 + 4 \omega_{\text{I}}^2 \tau_{\text{I}}^2} \quad (9)$$

$$\begin{aligned} g(\omega_{\text{I}}, \omega_{\text{S}}, \tau_{\text{I}}) = & \frac{\tau_{\text{I}}}{1 + (\omega_{\text{I}} - \omega_{\text{S}})^2 \tau_{\text{I}}^2} \\ & + \frac{3 \tau_{\text{I}}}{1 + \omega_{\text{I}}^2 \tau_{\text{I}}^2} + \frac{6 \tau_{\text{I}}}{1 + (\omega_{\text{I}} + \omega_{\text{S}})^2 \tau_{\text{I}}^2}. \quad (10) \end{aligned}$$

The temperature dependence of the correlation times τ_{I} (i = H, F) is expressed by an Arrhenius relationship as

$$\tau_{\text{I}} = \tau_{\text{I}}^0 \exp\left(\frac{E_{\text{ai}}}{RT}\right), \quad (11)$$

where E_{ai} the activation energy for the motions of the anions and cations, respectively.

The relaxation mechanism for 1000 K/ $T < 3.8$ is associated with the modulation of H–F dipolar interactions by reorientation of the [Sb(CH₃)₄][⊕] cation. Methyl group and isotropic PF₆[⊖] rotation are much too fast to influence the relaxation. Thus, the relaxation rates of the proton and fluorine nuclei have been

fitted according to (7) and (8) with τ_{H} and τ_{F} as the correlation time for isotropic [Sb(CH₃)₄][⊕] and isotropic PF₆[⊖] reorientation. The M_2 reductions are taken from the M_2 plateaus $M_2(^1\text{H}) = 7.8 \times 10^{-8} \text{ T}^2$ and $M_2(^{19}\text{F}) = 0.6 \times 10^{-8} \text{ T}^2$. The difference, $\Delta M_{2,\text{exp}} = 7.2 \times 10^{-8} \text{ T}^2$, is mainly determined by intraionic dipolar proton-proton interactions. Starting refinement runs with this initial value, the best fit to the experimental points is found to be given by $\Delta M_2(\text{HH}) = 6 \times 10^{-8} \text{ T}^2$ and additionally $\Delta M_2(\text{HF}) = 1.0 \times 10^{-8} \text{ T}^2$. Dipolar H–P interactions are too small to influence the relaxation curve, and therefore they are omitted. From the second moment reductions the relaxation constants

$$\begin{aligned} C_{\text{HH}} = 2/3 \gamma_{\text{H}}^2 \Delta M_2(\text{HH}) &= 2.87 \times 10^9 \text{ s}^{-2} \quad \text{and} \\ C_{\text{HF}} = 1/2 \gamma_{\text{H}}^2 \Delta M_2(\text{HF}) &= 3.58 \times 10^8 \text{ s}^{-2} \end{aligned}$$

have been obtained. The parameters describing thermally activated ¹H and ¹⁹F NMR spin lattice relaxation as obtained by least squares methods of (7) to (11) to the experimental $T_1(^1\text{H})$ values, using these relaxation constants, are listed in Table 4. In the fitting procedure a mean activation energy of 22.7 kJ/mol was inserted. As can be seen in Figs. 1 and 3, the resulting theoretical temperature dependence of both, proton and fluorine relaxation rates is in good agreement with the experimental T_1^{-1} values. The small deviation for $T > 325 \text{ K}$ is due to the onset of additional translational motion, which was not considered in the theoretical description.

Translational motion was also observed in the related compounds (NH₄)₃YF₆, Y = Ga, In [19]. As found by NMR and electrical conductivity measurements in these salts the anions as well as the cations undergo diffusion.

The activation energies calculated for both Larmor frequencies agree within the limits of error. The different correlation constants reflect the dependence of the relaxation rates on the Larmor frequency: the lower Larmor frequency (21.02 MHz) is correlated with the smaller correlation constants (Tabs. 4–6). The mean value of the activation energy for isotropic cation reorientation (22.7(25) kJ/mol) is in fairly good agreement with the respective value found in wideline measurements (18.1(10) kJ/mol) [3].

The energy for activating of [Sb(CH₃)₄][⊕] tumbling is small in comparison with values of other tetramethylstibonium salts as determined by ¹H NMR wide line and relaxation measurements [20].

Table 4. Parameters describing the isotropic Sb(CH₃)₄[⊕] tumbling in tetramethylstibonium hexafluorophosphate from least squares procedure of the proton spin lattice relaxation times according to (7) and (8) at high temperatures (standard deviation is given in brackets).

Isotropic Sb(CH ₃) ₄ [⊕] tumbling	$\omega_0/2\pi$ = 21.02 MHz	$\omega_0/2\pi$ = 36.55 MHz
Activation energy [kJ/mol]	23.5 (25)	21.8 (6)
Correlation time constant [10 ⁻¹¹ s]	2.14 (55)	4.75 (31)
Relaxation constant C_{HH} [s ⁻²]	2.87 × 10 ⁹	
Relaxation constant C_{HF} [s ⁻²]	3.58 × 10 ⁸	
Temperature range	217 < T/K < 357	

Relaxation Behaviour at Intermediate Temperatures

For 1000 K/T > 4.6 the spin lattice relaxation times are determined mainly by the PF₆[⊖] reorientation mechanism. It is assumed that isotropic cation reorientation is too slow and methyl group rotation too fast to influence the relaxation. In this case single exponential relaxation would be expected, and this is observed in the experiment. The small deviations from single exponential relaxation behaviour in the temperature interval 205 < T/K < 240 can be explained by the change in the relaxation determining motion (isotropic cation tumbling ↔ isotropic anion tumbling). H–F dipolar interactions are quite small and the relaxation rate is given by

$$\begin{aligned} \frac{1}{T_1(^{19}\text{F})} = & \frac{2}{3} \gamma_F^2 \Delta M_2(\text{FF}) g(\omega_F, \tau_F) \\ & + \frac{1}{2} \gamma_F^2 \Delta M_2(\text{FH}) g(\omega_F, \omega_H, \tau_F) \\ & + \frac{1}{2} \gamma_F^2 \Delta M_2(\text{FP}) g(\omega_F, \omega_P, \tau_F) \quad (12) \end{aligned}$$

The proton spin lattice relaxation rate 1/T₁(¹H) is determined mainly by random modulation of H–F dipolar interactions due to PF₆[⊖] reorientations. Therefore,

$$\begin{aligned} \frac{1}{T_1(^1\text{H})} = & \frac{1}{2} \gamma_H^2 \Delta M_2(\text{HF}) g(\omega_H, \omega_F, \tau_F) \\ & + \frac{1}{2} \gamma_H^2 \Delta M_2(\text{HP}) g(\omega_H, \omega_P, \tau_F). \quad (13) \end{aligned}$$

The spectral density functions and second moment reductions are defined in the same manner as above (see (9) and (10)), but they are determined by PF₆[⊖]

reorientations; τ_F is the correlation time of the isotropic anion reorientation.

In the temperature range 100 > T/K > 83 there is nearly a linear relation between the logarithmic form of the relaxation rates of both, proton and fluorine nuclei and the inverse temperature. The relation of the rates measured is proportional to the squared inverse fraction of the Larmor frequencies (36.55 MHz/21.02 MHz)² = 3.0:

¹H NMR, T ≈ 91 K:

$$\begin{aligned} T_1^{-1}(21.02 \text{ MHz})/T_1^{-1}(36.55 \text{ MHz}) \\ = 1.9960 \text{ s}^{-1}/0.6793 \text{ s}^{-1} = 2.9; \end{aligned}$$

¹⁹F NMR, T ≈ 93 K:

$$\begin{aligned} T_1^{-1}(21.02 \text{ MHz})/T_1^{-1}(36.55 \text{ MHz}) \\ = 5.5865 \text{ s}^{-1}/1.8399 \text{ s}^{-1} = 3.0. \end{aligned}$$

Thus, the following conditions must be valid on the low temperature side of the maxima caused by isotropic anion reorientation:

$$\begin{aligned} \omega \tau_F \gg 1 \quad (\omega = \omega_F \simeq \omega_H \simeq \omega_P) \quad \text{and} \\ (\omega_F - \omega)^2 \ll \omega_F^2 \quad (\omega = \omega_H, \omega_P). \end{aligned}$$

Using the experimental M₂(¹⁹F) reduction 5.4 × 10⁻⁸ T² as initial value, refinement runs yield the second moment reductions ΔM₂(FF) = 5.1 × 10⁻⁸ T², ΔM₂(FP) = 1.0 × 10⁻⁸ T², and ΔM₂(FH) = 2.0 × 10⁻⁸ T². The results of the least squares procedure of the fluorine relaxation rates are given in Table 5.

For both nuclei investigated the agreement the calculated (lines in Figs. 1 and 3) and measured relaxation rates is good. A mean value of 10.4(11) kJ/mol for the activation energy for isotropic anion tumbling is obtained from the measurements at the two Larmor frequencies. The different values for the correlation time constant reflect the frequency dependence of T₁⁻¹(¹⁹F) and T₁⁻¹(¹H) in the right way: the higher Larmor frequency is correlated with a smaller relaxation time constant and a smaller relaxation rate at a given temperature.

The increase of the relaxation rates of the fluorine spin system at 1000 K/T > 13 can be explained by a further reorientational motion of the hexafluorophosphate anion: from the results of the M₂ measurements this is known to be the uniaxial anion reorientation. The theoretical relaxation rates are calculated using the same equations as in the case of the isotropic anion motion. Below 38 K the motion of the ¹⁹F spin system is too slow to influence the relaxation, the

Table 5. Parameters describing the isotropic PF₆[⊖] tumbling in tetramethylstibonium hexafluorophosphate from least squares procedure of the fluorine spin lattice relaxation times according to (12) and (13) at intermediate temperatures (standard deviation is given in brackets).

Isotropic PF ₆ [⊖] tumbling	$\omega_0/2\pi$ = 21.02 MHz	$\omega_0/2\pi$ = 36.55 MHz
Activation energy [kJ/mol]	10.8 (7)	10.1 (11)
Correlation time constant [10 ⁻¹² s]	1.51 (12)	3.21 (39)
Relaxation constant C_{FF} [s ⁻²]	2.15 × 10 ⁹	
Relaxation constant C_{FP} [s ⁻²]	3.17 × 10 ⁸	
Relaxation constant C_{FH} [s ⁻²]	6.34 × 10 ⁸	
Temperature range	83 < T/K < 212	

Table 6. Parameters describing the uniaxial PF₆[⊖] reorientation in tetramethylstibonium hexafluorophosphate from least squares procedure of the fluorine spin lattice relaxation times according to (12) and (13) at intermediate temperatures (standard deviation is given in brackets).

Uniaxial PF ₆ [⊖] reorientation	$\omega_0/2\pi$ = 21.02 MHz	$\omega_0/2\pi$ = 36.55 MHz
Activation energy [kJ/mol]	5.6 (8)	6.0 (5)
Correlation time constant [10 ⁻¹⁵ s]	1.71 (16)	2.46 (15)
Relaxation constant C_{FF} [s ⁻²]	2.07 × 10 ⁹	
Relaxation constant C_{FP} [s ⁻²]	3.80 × 10 ⁸	
Relaxation constant C_{FH} [s ⁻²]	2.85 × 10 ⁸	
Temperature range	33 < T/K < 69	

anion motion is frozen in and the ¹⁹F relaxation rates increase again on lowering the temperature.

The determination of the activation parameters of the uniaxial anion rotation can be done from both, the linear portion of the high temperature side of the maximum in the interval 69 > T/K > 50 and from the low temperature side (39 > T/K > 33). The first option is used for measurements at 21.02 MHz (closed symbols in Fig. 4) and the second one for experimental points at 36.55 MHz Larmor frequency (open symbols in Fig. 4). In both cases the second moment reductions $\Delta M_2(\text{FF}) = 4.9 \times 10^{-8} \text{ T}^2$, $\Delta M_2(\text{FH}) = 1.2 \times 10^{-8} \text{ T}^2$, and $\Delta M_2(\text{FP}) = 0.9 \times 10^{-8} \text{ T}^2$, obtained by refinement runs with the initial value from experimental second moment reduction, were employed. Parameters for uniaxial anion reorientation as obtained from least squares fit of (12) and (13) are given in Table 6.

The activation energies as obtained from the high and low temperature side of the maximum of the relaxation rate agree within limits of error and confirm the assumptions made. The mean value for uniaxial PF₆[⊖] rotation is 5.8(8) kJ/mol; it is half the value for isotropic anion reorientation.

A clear distinction between two-, three-, or fourfold rotation of the hexafluorophosphate anion can not be done by the spin-lattice relaxation measurements. The second moment of a rigid isolated PF₆ octahedron with d(F...F) = 223.4 pm is $12.2 \times 10^{-8} \text{ T}^2$ [3]. The experimental value at 7.6 K nearly matches: $M_2(^{19}\text{F}) = 11.40(57) \times 10^{-8} \text{ T}^2$. Since there are no interionic contributions considered in the theoretical value, it may be assumed that the mean F...F distance is greater than 223.4 pm. The determination of the spin lattice relaxation rates by the onset of the uniaxial anion rotation has been described using the second moment reductions of the F–H, F–P, and F–F dipo-

lar interactions ($1.2 \times 10^{-8} \text{ T}^2$, $0.9 \times 10^{-8} \text{ T}^2$, and $4.9 \times 10^{-8} \text{ T}^2$, respectively). Subtracting these values from the maximal experimental second moment results in $M_2(^{19}\text{F}) = 4.97 \times 10^{-8} \text{ T}^2$, a plateau which should correspond to the uniaxial rotation state. Since the experimental value is $(6.5 \cdots 7.2) \times 10^{-8} \text{ T}^2$, the difference is $> 1.5 \times 10^{-8} \text{ T}^2$. Starting on the other side from an experimental value $M_2(^{19}\text{F}) = 7.2 \times 10^{-8} \text{ T}^2$ for uniaxial rotation, consideration of the second moment reductions for onset of the isotropic anion tumbling ($\Delta M_2(\text{FP}) = 1.0 \times 10^{-8} \text{ T}^2$, $\Delta M_2(\text{FF}) = 5.1 \times 10^{-8} \text{ T}^2$) results in $M_2(^{19}\text{F}) = 1.1 \times 10^{-8} \text{ T}^2$ which is smaller than the experimental value ($1.40 \times 10^{-8} \text{ T}^2$).

Thus, for both transitions (stationary PF₆[⊖] group → uniaxial PF₆[⊖] rotation; uniaxial PF₆[⊖] rotation → isotropic PF₆[⊖] reorientation) there are deficits, which may depend on the distortion of the anion and/or the detailed arrangement of the fluorine nuclei to the methyl groups of the cation. Because of the lack of the point positions of P and F the symmetry axis of the uniaxial anion rotation can not be determined. Nevertheless, the proton and fluorine relaxation rates can only be described correctly if a reduction of the dipolar F–P interaction is considered. This contribution consists mainly of intra-PF₆[⊖] interactions. In the state of isotropic anion rotation the intraionic F–P contribution is reduced to zero and the M_2 reduction of the F–P interaction is identical with $M_2(\text{F–P})$ in the case of uniaxial rotation. Therefore a rotation about the threefold axis, where the intraionic $M_2(\text{F–P})$ is zero, seems to be not very probable.

A similar rotational behaviour and mechanism of the freezing-in process of a complex anion octahedron via uniaxial rotation was found in [N(C₂H₅)₄]₂SbF₆ [21]: reorientation takes place at $\approx 50 \text{ K}$ about a fourfold symmetry axis with activation energies of 27.6

kJ/mol for isotropical and 24.3 kJ/mol for C_4 rotation of SbF_6^\ominus .

In contrast to the alkali metal hexafluorophosphates a phase transition could not be detected for $[\text{Sb}(\text{CH}_3)_4]\text{PF}_6$ by differential thermal analysis (DTA) in the range $77 < T/\text{K} < 330$. The phase transition of the alkali metal compounds occurs in the temperature range where PF_6^\ominus reorients isotropically. At very low temperatures the PF_6^\ominus reorientation is freezing in; an uniaxial motional state as in the $[\text{Sb}(\text{CH}_3)_4]^\oplus$ compound was not observed [9, 22]. Since the relaxation rates of APF_6 , $A = \text{K}, \text{Rb}$, depend strongly on the sample treatment before the measurements [9], the activation energies for PF_6^\ominus tumbling are not very well determined. Omitting therefore $A = \text{K}, \text{Rb}$, the activation energies of the isotropic PF_6 motion in APF_6 decreases with increasing cation size in the order $A = \text{Na} > \text{NH}_4 > \text{Sb}(\text{CH}_3)_4$ (28.9, 18.4, 10.4 kJ/mol, respectively). This can be rationalized by the decrease of contact areas of close-packed spheres if the size of the cation sphere increases.

It is interesting that $[\text{Sb}(\text{CH}_3)_4]\text{PF}_6$ shows a similar relaxation behaviour to $[\text{Sb}(\text{CH}_3)_4]_2\text{SiF}_6$ for $T > 125 \text{ K}$, and both again show different behaviour to the series $[\text{M}(\text{CH}_3)_4]_2\text{SiF}_6$ with $M = \text{N}, \text{P}, \text{As}$ [5]. Two flat minima were found for $T_1(^1\text{H})$ in $[\text{Sb}(\text{CH}_3)_4]_2\text{SiF}_6$ with $M = \text{N}, \text{P}, \text{As}$ [5]. Two flat minima were found for $T_1(^1\text{H})$ in $[\text{Sb}(\text{CH}_3)_4]_2\text{SiF}_6$ and have been suggested to be due to crystallographically inequivalent methyl groups, whereas the $T_1(^{19}\text{F})$ temperature dependence could not be described satisfactorily.

Comparison with the compound investigated in this study shows that the temperature dependence in this temperature range is also influenced by the third term of (12), which leads in the case of $[\text{Sb}(\text{CH}_3)_4]\text{PF}_6$ to maxima in $1/T_1(^{19}\text{F})$ and $1/T_1(^1\text{H})$ with shoulders on the low and high temperature side, respectively. The same term should also be responsible for the relaxation curves of $[\text{Sb}(\text{CH}_3)_4]_2\text{SiF}_6$, where the extrema and shoulders are formed weaker.

Rotational Tunneling of the Methyl Groups

In the low temperature range the motional spectrum of the methyl groups is dominated by quantum mechanical tunneling. The tunnel splittings of the torsional ground states of the two crystallographic methyl groups and their temperature dependences are not known and therefore a quantitative description of the relaxation behaviour is not possible. Nevertheless,

since there is a remarkable similarity to the $T_1^{-1}(^1\text{H}) = f(T)$ diagram of tetramethylstibonium iodide, a qualitative description can be given by comparing both compounds, $[\text{Sb}(\text{CH}_3)_4]\text{I}$ and $[\text{Sb}(\text{CH}_3)_4]\text{PF}_6$.

The X-ray structure analysis reveals that the cations of both compounds consist of a distorted tetrahedron with two crystallographically inequivalent methyl groups in the ratio of occurrence $\text{CH}_3(1):\text{CH}_3(2) = 3:1$. The bond length $\text{Sb}-\text{C}$ of the more frequent $\text{CH}_3(1)$ groups in a cation is smaller than of the unique $\text{CH}_3(2)$. In the fixed window diagrams of both compounds, tetramethylstibonium iodide (Fig. 3 of [4]) and tetramethylstibonium hexafluorophosphate (Fig. 9), 2 steps occur. Thus, the rotational potential and the relaxation behaviour of the methyl groups of the two tetramethylstibonium salts are assumed to be similar. The maximum of the proton relaxation rate at $T = 39 \text{ K}$ in Fig. 2 may then be attributed to $\text{CH}_3(2)$ of the hexafluorophosphate compound, and $\text{CH}_3(1)$ determines the spin lattice relaxation below $T = 18 \text{ K}$. From the temperature dependence in the interval $45 < T/\text{K} < 25$ it may be deduced that the two maxima which are caused by the transition within the twofold degenerated E states (E_A and E_B) and the symmetry changing transition from A to E of the sublevels of the torsional ground state are close together [14, 23]. The Larmor frequency dependent part of the $T_1(^1\text{H}) = f(T)$ curve at the low temperature side coincides with the frequency dependent part lying on the high temperature side of the curve. The frequency dependence of $T_1(^1\text{H})$ in the range $40 < 1000 \text{ K}/T < 55$ is small; it is assumed to be the result of the overlap of the $T_1(^1\text{H})$ contributions of the two crystallographically inequivalent methyl groups to the resulting observable $T_1(^1\text{H})$.

Because of the deviation from classical behaviour and because no tunneling assisted maxima occurred it can be deduced that the tunneling splittings must be larger than the Larmor frequency and the rotational barrier must be small for both methyl groups in tetramethylstibonium hexafluorophosphate.

From the temperatures $T_{1/2}$ in the fixed window diagram the apparent activation energies of the potential can be estimated: the correlation frequencies for the rotational tunneling of methyl groups usually lie in the order of $\approx 10^{12} \text{ s}^{-1}$ [2]. Regarding the CH_3 groups of $\text{Sn}(\text{CH}_3)_4$ [1] and $[\text{Sb}(\text{CH}_3)_4]\text{I}$ [4], where there are two crystallographically inequivalent methyl groups in the ratio $\text{CH}_3(1):\text{CH}_3(2) = 3:1$ as in $[\text{Sb}(\text{CH}_3)_4]\text{PF}_6$; the respective correlation frequencies

are $\tau(1) = 4.0 \times 10^{-13}$ s ($\text{Sn}(\text{CH}_3)_4$) and $\tau(1) = 0.15 \times 10^{-13}$ s ($[\text{Sb}(\text{CH}_3)_4]\text{I}$). As mentioned above, the $\text{CH}_3(1)$ groups of $[\text{Sb}(\text{CH}_3)_4]\text{PF}_6$ should behave similar and their relaxation constant is assumed to lie within $0.15 < \tau(1) \times 10^{13}/\text{s} < 0.40$. With $T_{1/2} = 17.0$ K an apparent activation energy of the $\text{CH}_3(1)$ groups $1.70 < E_H(1)/\text{kJ/mol} < 1.22$ is estimated for $[\text{Sb}(\text{CH}_3)_4]\text{PF}_6$.

The same procedure with $\tau(2) = 0.6 \times 10^{-13}$ s and $\tau(2) = 2.2 \times 10^{-13}$ s for $\text{Sn}(\text{CH}_3)_4$ [1] and $[\text{Sb}(\text{CH}_3)_4]\text{I}$ [4], respectively, and $T_{1/2} = 46.0$ K (see Fig. 9) yields

$3.50 < E_H(2)/\text{kJ/mol} < 3.99$ for the apparent activation energy of the $\text{CH}_3(2)$ groups in the hexafluorophosphate salt.

Acknowledgement

The help of Dr. S. Mahling-Ennaoui at the ILL is gratefully acknowledged. This work was supported by the Bundesministerium für Forschung und Technologie (project no. 03-WS2DAR-9).

- [1] M. Prager, K.-H. Duprée, and W. Müller-Warmuth, *Z. Phys.* **B 51**, 309 (1983).
- [2] M. Prager and W. Müller-Warmuth, *Z. Naturforsch.* **39a**, 1187 (1984).
- [3] G. Burbach, S. Dou, and Al. Weiss, *Ber. Bunsenges. Phys. Chem.* **93**, 1302 (1989).
- [4] G. Burbach and Al. Weiss, *Z. Naturforsch.* **46a**, 759 (1991).
- [5] H. Rager and Al. Weiss, *Ber. Bunsenges. Phys. Chem.* **82**, 535 (1978).
- [6] S. Sato, M. Kondo, R. Ikeda, and D. Nakamura, *Ber. Bunsenges. Phys. Chem.* **93**, 450 (1989).
- [7] E. C. Reynhardt, J. C. Pratt, and A. Watton, *J. Phys. C: Solid State Phys.* **19**, 919 (1986).
- [8] S. Takeda, T. Fujiwara, and H. Chihara, *J. Phys. Soc. Japan* **58**, 1793 (1989).
- [9] H. S. Gutowsky and S. Albert, *J. Chem. Phys.* **58**, 5446 (1973).
- [10] M. Sass and D. Ziessow, *J. Magn. Reson.* **25**, 263 (1977).
- [11] F. N. H. Robinson, *J. Phys. C: Sci. Instrum.* **15**, 814 (1982).
- [12] E. R. Andrew, *Phys. Rev.* **91**, 425 (1953).
- [13] S. Albert and H. S. Gutowsky, *J. Chem. Phys.* **59**, 3585 (1973).
- [14] D. Cavagnat, *J. Chim. Phys.* **82**, 239 (1985).
- [15] W. Schwarz and H.-J. Guder, *Z. Anorg. Allg. Chem.* **444**, 105 (1978).
- [16] A. F. Wells, *Z. Kristallogr.* **99**, 367 (1938).
- [17] J. Timmermans, *Bull. Soc. Chim. Belge* **44**, 17 (1935).
- [18] A. Abragam, *The Principles of Nuclear Magnetism*, Clarendon Press, Oxford 1961.
- [19] A. Sasaki, Y. Furukawa, and D. Nakamura, *Ber. Bunsenges. Phys. Chem.* **93**, 1142 (1989).
- [20] G. Burbach, Dr.-Ing. thesis, Darmstadt 1992.
- [21] E. C. Reynhardt and J. P. S. Rash, *J. Magn. Reson.* **42**, 88 (1981).
- [22] G. R. Müller and H. S. Gutowsky, *J. Chem. Phys.* **39**, 1983 (1963).
- [23] W. Müller-Warmuth, R. Schüler, M. Prager, and A. Kollmar, *J. Chem. Phys.* **69**, 2382 (1978).